The current issue and full text archive of this journal is available on Emerald Insight at:
https://www.emerald.com/insight/0332-1649.htm

Eddy current losses in power voltage transformer open-type cores

Stjepan Frljić, Bojan Trkulja and Ana Drandić
Faculty of Electrical Engineering and Computing, University of Zagreb, Zagreb, Croatia

Received 13 January 2023
Revised 28 June 2023
Accepted 19 August 2023

Abstract

Purpose – The purpose of this paper is to present a methodology for calculating eddy current losses in the core of a single-phase power voltage transformer, which, unlike a standard power transformer, has an open-type core (I-type core). In those apparatus, reduction of core losses is achieved by using a multipart open-type core that is created by merging a larger number of leaner cores.

Design/methodology/approach – 3D FEM approach for calculation of eddy current losses in open-type cores based on a weak $A\lambda A$ formulation is presented. Method in which redundant degrees of freedom are eliminated is shown. This enables faster convergence of the simulation. The results are benchmarked using simulations with standard AVA formulation.

Findings – Results using weak $A\lambda A$ formulation with elimination of redundant degrees of freedom are in agreement with both simulation using only weak $A\lambda A$ formulation and with simulation based on AVA formulation.

Research limitations/implications – The presented methodology is valid in linear cases, whereas the nonlinear case will be part of future work.

Practical implications – Presented procedure can be used for the optimization when designing the open-type core of apparatus like power voltage transformers.

Originality/value – The presented method is specifically adapted for calculating eddy currents in the open-type core. The method is based on a weak formulation for the magnetic vector potential A and the current vector potential λ, incorporating numerical homogenization and a straightforward elimination of redundant degrees of freedom, resulting in faster convergence of the simulation.

Keywords Eddy currents, FEM, Transformers, Finite element method

Paper type Research paper

1. Introduction

A power voltage transformer is a power transformer with an open-type laminated core, which is particularly suitable for powering the power plant's own consumption and for electrifying areas where there is no distribution network (Ziger *et al.*, 2018). Power transformers with open-type core offer several additional advantages over power transformers with conventional cores. These include simpler manufacturing, enhanced robustness, explosion-proof safety, reduced weight and significantly lower ferroresonance (Ziger *et al.*, 2014; Lapthorn and Keenan, 2015). The use of the open-type core in combination with superconducting windings is being explored

This work has been fully supported by Croatian Science Foundation under the project number IP-2020-02-2369.

COMPEL - The international journal for computation and mathematics in electrical and electronic engineering
Vol. 42 No. 5, 2023
pp. 1039-1051
Emerald Publishing Limited
0332-1649
DOI 10.1108/COMPEL-01-2023-0016

to reduce losses in windings (Liew and Bodger, 2001). A comparison of an open-type core transformer and a transformer with conventional core is shown in Figure 1.

In the conventional core [Figure 1(a)], most of the magnetic flux remains within the core, resulting in negligible stray flux. Eddy currents are predominantly induced by the tangential magnetic flux on the lamination surfaces, forming narrow loops within the laminations. These localized eddy currents can be treated as a 1D phenomenon, as discussed in Dular *et al.* (2003) and Gyselinck *et al.* (1999). To account for edge effects, analytical homogenization methods are proposed in Hollaus and Schöberl (2015) and Hollaus and Schoberl (2018) using a multiscale approach with micro-shape functions. In addition, a multiscale modeling approach, incorporating both eddy currents and hysteresis, is presented in Niyonzima *et al.* (2013). The method described in Henrotte *et al.* (2015) uses algebraic approximation to determine material characteristics, with parameters obtained in the initial stage of the simulation for each finite element in the mesh.

In certain situations, the stray magnetic flux is not negligible, so in addition to the eddy currents induced by the main magnetic flux, it is also necessary to model the eddy currents induced by the stray magnetic flux, which usually flow in large loops tangential to the lamination surfaces (De Gersem *et al.*, 2012).

In the case of the open-type core shown in Figure 1(b), all the magnetic flux from the core passes through the core/air interface and a large part of the magnetic flux is perpendicular to the lamination surfaces. Therefore, the induced planar eddy currents forming wide loops take on significant values (Bíró *et al.*, 2005). A multiscale approach that also considers planar eddy currents using asymmetric micro-shape functions is presented in Hanser *et al.* (2022).

This paper presents a 3D FEM approach for calculation of eddy current losses in open-type cores based on a weak $A\tau A$ formulation. The results are verified by comparison with simulations based on standard AVA formulation.

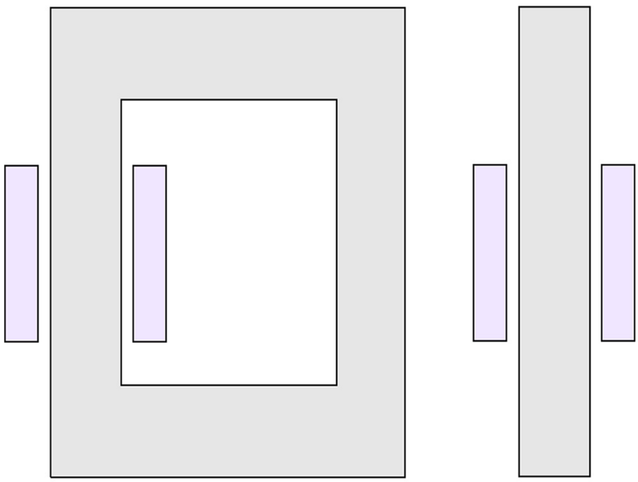

Figure 1.
Comparison between an open-type core and a conventional core

Notes: (a) Cross section of the conventional core and the associated cylindrical winding; (b) cross section of an open-type core and its associated cylindrical winding
Source: Authors' own work

2. Problem definition

Problem domain Ω consists of the core region Ω_c, air region Ω_0 and the winding region Ω_s in which the source current J_s flows, as shown in Figure 2. Region Ω_c has the characteristics of an electrically conductive ferromagnetic material. Linear characteristics of the material in Ω_c are assumed in the presented work. In addition, a sinusoidal time dependence of the source current in the low-frequency range is assumed, so the set of quasi-static Maxwell's equations in Ω_c is:

$$\nabla \times \rho \boldsymbol{J} = -j\omega \boldsymbol{B} \tag{1}$$

$$\nabla \times \nu \boldsymbol{B} = \boldsymbol{J} \tag{2}$$

$$\nabla \cdot \boldsymbol{B} = 0 \tag{3}$$

$$\nabla \cdot \boldsymbol{J} = 0, \tag{4}$$

where $\boldsymbol{B}$ represents the vector field of magnetic induction, $\boldsymbol{J}$ represents the vector field of eddy current density, ω represents the frequency and j is the imaginary unit. Parameter ρ represents the electrical resistivity of the material and is equal to the reciprocal of the electrical conductivity σ, whereas ν represents the magnetic reluctivity of the material and is equal to the reciprocal of the magnetic permeability μ.

As the emphasis in the presented work is on the calculation of losses due to eddy currents exclusively in Ω_c, region Ω_s is defaulted as nonmagnetic and electrically nonconductive as the region Ω_0.

Consequently, for electrical conductivity in Ω_0 and Ω_s, it is valid that $\sigma = 0$, and for magnetic permeability, it is valid that $\mu = \mu_0$. Therefore, the set of quasi-static Maxwell's equations in Ω_0 and Ω_s is:

$$\nabla \times \nu_0 \boldsymbol{B} = \boldsymbol{J_s} \tag{5}$$

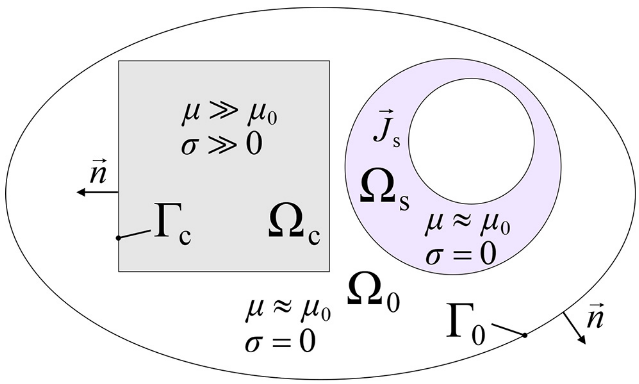

Source: Authors' own work

Figure 2.
Problem domain with associated subdomains

$$\nabla \cdot \boldsymbol{B} = 0 \tag{6}$$

$$\nabla \cdot \boldsymbol{J_s} = 0, \tag{7}$$

where $\boldsymbol{B}$ represents the vector field of magnetic induction, $\boldsymbol{J_s}$ represents the given source current density vector field and ν_0 represents the magnetic reluctivity of the vacuum for which it is valid that $\nu_0 = \mu_0^{-1}$.

3. Eddy currents in laminated core

As the region Ω_c is laminated, magnetic induction vector $\boldsymbol{B}$ and the eddy current density vector $\boldsymbol{J}$ can be disassembled into components in local $\alpha\beta\gamma$-coordinate system of each individual lamination, where α-direction and β-direction are tangential to the lamination surface, whereas γ-direction is perpendicular to the lamination surface, as shown in Figure 3.

By disassembling the magnetic induction $\boldsymbol{B}$ into its components, we get the sum:

$$\boldsymbol{B} = \boldsymbol{B_{\alpha\beta}} + \boldsymbol{B_\gamma}, \tag{8}$$

where $\boldsymbol{B_{\alpha\beta}}$ represents tangential and $\boldsymbol{B_\gamma}$ represents normal component of magnetic induction $\boldsymbol{B}$. According to equation (1), each of the components induces eddy currents inside the laminations, i.e. it holds:

$$\nabla \times \rho \boldsymbol{J_{\alpha\beta\gamma}} = -j\omega \boldsymbol{B_{\alpha\beta}} \tag{9}$$

$$\nabla \times \rho \boldsymbol{J_{\alpha\beta}} = -j\omega \boldsymbol{B_\gamma}, \tag{10}$$

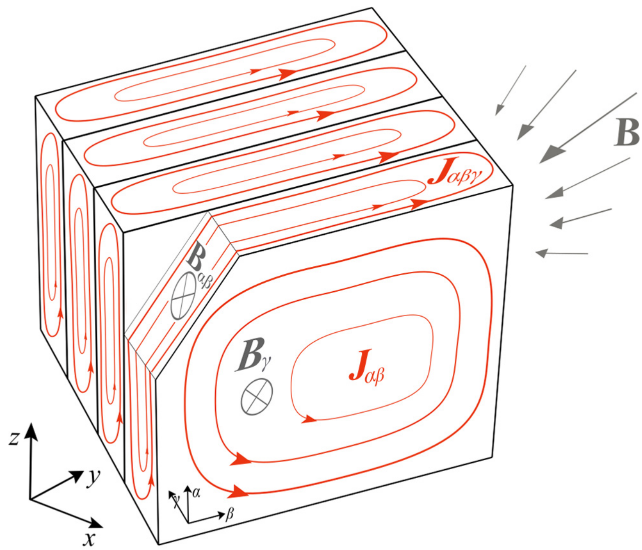

Figure 3.
Eddy currents in a laminated medium

Source: Authors' own work

where $\boldsymbol{J}_{\alpha\beta\gamma}$ represents the density of narrow loops of eddy currents that are induced by the tangential component of the magnetic induction $\boldsymbol{B}_{\alpha\beta}$, whereas $\boldsymbol{J}_{\alpha\beta}$ represents the density of large eddy current loops that are induced by the normal component of the magnetic induction $\boldsymbol{B}_{\gamma}$, as presented in Figure 3.

Finally, for the total current density $\boldsymbol{J}$ it is valid:

$$\boldsymbol{J} = \boldsymbol{J}_{\alpha\beta\gamma} + \boldsymbol{J}_{\alpha\beta} \tag{11}$$

If for each lamination it is true that its thickness d is much smaller than its width l and height h, i.e. $d \ll l$ and $d \ll h$, then it holds:

$$\int_{\Omega_L} \boldsymbol{J}_{\alpha\beta} \cdot \boldsymbol{J}_{\alpha\beta\gamma} dV \approx 0, \tag{12}$$

where Ω_{L} denotes the region of one lamination sheet. Equation (12) indicates that $\boldsymbol{J}_{\alpha\beta\gamma}$ and $\boldsymbol{J}_{\alpha\beta}$ are approximately orthogonal, so it is then possible to calculate the losses $P_{\alpha\beta\gamma}$ due to eddy currents $\boldsymbol{J}_{\alpha\beta\gamma}$ separately from the losses $P_{\alpha\beta}$ due to eddy currents $\boldsymbol{J}_{\alpha\beta}$, i.e. the total losses P can be calculated as:

$$P = P_{\alpha\beta\gamma} + P_{\alpha\beta} \tag{13}$$

4. Homogenization procedure

The laminated core is made of very thin laminations insulated from each other by even thinner layers of insulation. A direct consequence of the rapidly changing material characteristics is the highly oscillatory spatial dependence of the eddy current density $\boldsymbol{J}_{\alpha\beta\gamma}$. Consequently, an exceedingly dense mesh with multiple layers of finite elements per unit thickness of a single lamination sheet is necessary to correctly model the characteristics of the material, especially the field $\boldsymbol{J}_{\alpha\beta\gamma}$, which is not permissible in a practical 3D case. To enable the application of a coarse mesh, where the finite elements are wide enough to encompass parts of several neighboring lamination sheets, homogenization is needed (Kaimori *et al.*, 2007). In the case of low frequencies, it is a reasonable approximation to assume that $\boldsymbol{B}_{\alpha\beta}$ remains constant across the thickness of a lamination sheet. In that case, by using equation (9), it becomes possible to explicitly express $\boldsymbol{J}_{\alpha\beta\gamma}$ in terms of $\boldsymbol{B}_{\alpha\beta}$, as demonstrated in Ziger *et al.* (2014). Consequently, the weak formulation term associated with $\boldsymbol{J}_{\alpha\beta\gamma}$ is modeled using $\boldsymbol{B}_{\alpha\beta}$. As $\boldsymbol{B}_{\alpha\beta}$ exhibits a monotonic behavior in the region of neighboring lamination sheets, the utilization of a coarse mesh is permissible. In this paper, the contribution of $\boldsymbol{J}_{\alpha\beta\gamma}$ in the 3D weak formulation will also be considered by using $\boldsymbol{B}_{\alpha\beta}$, but this transformation will be determined numerically through a 2D simulation in the preprocessing stage. Therefore, similar to Ziger *et al.* (2014), for the homogenized magnetic reluctivity tensor $\boldsymbol{\nu}$ follows $\boldsymbol{\nu} = \mathrm{Re}\{\boldsymbol{\nu}\} + \mathrm{jIm}\{\boldsymbol{\nu}\}$. Accordingly, the diagonal tensors that will define the characteristics of the new homogenized material are as follows:

$$\boldsymbol{\rho} = \begin{bmatrix} \rho_\alpha & \rho_\beta & \rho_\gamma \end{bmatrix} \tag{14}$$

$$\boldsymbol{\nu} = \begin{bmatrix} \nu_\alpha & \nu_\beta & \nu_\gamma \end{bmatrix} + j\begin{bmatrix} 0 & \kappa & \kappa \end{bmatrix}, \tag{15}$$

where individual components are calculated as:

$$\rho_\alpha = \rho_\beta = \rho K_f \tag{16}$$

$$\rho_\gamma^{-1} \approx 0 \tag{17}$$

$$\nu_\alpha^{-1} = \nu_\beta^{-1} = \nu^{-1} K_f + \nu_0^{-1}\left(1 - K_f\right) \tag{18}$$

$$\nu_\gamma = \nu K_f + \nu_0\left(1 - K_f\right), \tag{19}$$

where K_f is filling factor of a given laminated core. It remains to determine the parameter κ using the numerical homogenization procedure.

4.1 Calculation of the parameter κ

Parameter κ is determined numerically, in the preprocessing phase, by means of a 2D simulation of eddy currents. For 2D simulation, the weak AT-formulation described in Henrotte *et al.* (2015) is used. The value of average induction $\overline{\boldsymbol{B}}_{2D}$ is given as source, and after the simulation is completed, a 2D vector field $\boldsymbol{J}_{2D}$ is obtained that represents eddy currents $\boldsymbol{J}_{\alpha\beta\gamma}$ within cross section of i-th finite element, as can be seen in Figure 4. Finally, using the expression:

$$\kappa_i = \int_{S_i} \rho \boldsymbol{J}_{2D}^2 dS \Big/ \int_{S_i} \omega \overline{\boldsymbol{B}}_{2D}^2 dS \tag{20}$$

κ_i is obtained, where index i denotes the i-th finite element of the coarse mesh, with the surface S_i, marked with dashes in Figure 4. Surface S_i represents the surface of the cross-section through the i-th finite element of the 3D structural mesh. Therefore, κ is a discrete spatial function with a constant value within the i-th FE of the 3D structural coarse mesh. As can be seen in Figure 4, the parameter κ considers edge effects. The size of the coarse

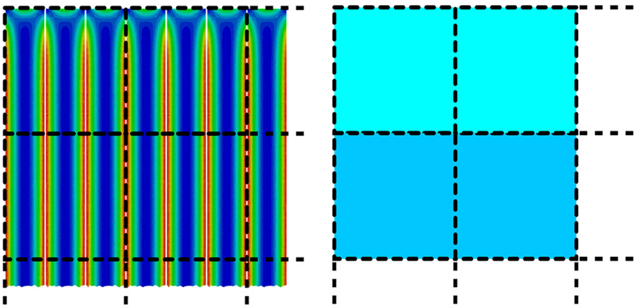

Notes: (a) Current density obtained by 2D simulation J2D. The dashed rectangles indicate the cross sections of the 3D finite elements of the coarse mesh; (b) display of discrete values of parameter κ in different finite elements
Source: Authors' own work

Figure 4. Calculation of the parameter κ in the preprocessing phase

mesh finite element affects the value of κ at the edges of the laminations. The value of κ coincides with the value obtained through an analytical approach presented in Ziger *et al.* (2014).

The region Ω_c is homogenized, i.e. Faraday's equation (9) in 3D weak formulation will be considered indirectly via equation (15) in combination with equations (18)–(20). Also, by equations (14), (16) and (17), a new material disables currents in the γ-direction to prevent inducing currents $\boldsymbol{J}_{\alpha\beta\gamma}$. Thus, $\boldsymbol{B}$ can be used instead of $\boldsymbol{B}_\gamma$ in (10), i.e:

$$\nabla \times \rho \boldsymbol{J}_{\alpha\beta} = -j\omega \boldsymbol{B} \tag{21}$$

On the other hand, from the combination of equations (2) and (11), it follows:

$$\nabla \times \nu \boldsymbol{B} = \boldsymbol{J}_{\alpha\beta} + \boldsymbol{J}_{\alpha\beta\gamma} \tag{22}$$

noting that $\boldsymbol{J}_{\alpha\beta\gamma}$ in the 3D weak formulation will be accounted for indirectly, via $\boldsymbol{B}$, by using $\boldsymbol{\nu}$ instead of ν.

5. Multipart open-type cores

As the open-type core represents a magnetic circuit with a large air gap, the magnetic voltage drop in the air is dominant. Consequently, the magnetic flux significantly enters the core perpendicular to the lamination surfaces, inducing large eddy current loops as shown in Figure 3. In the case of open-type cores whose lamination sheets have large dimensions (thickness $\sim$ 0.35 mm, width $>$ 5 cm and height $>$ 50 cm), losses due to large loops of eddy currents induced by the magnetic flux perpendicular to the lamination surface are significant. Therefore, to further reduce core losses, it is technologically feasible to build a core from a larger number of leaner cores. A cross section of one such core is shown in Figure 5(b). The two-part core shown in Figure 5(b) has lower losses than the standard one-part core shown in Figure 5(a) due to the reduction in the area of the lamination sheets.

6. Weak formulation

A formulation based on the magnetic vector potential $\boldsymbol{A}$ and the electric scalar potential V is often used to model eddy currents. However, this formulation is not desirable in the case of a multipart open-type core due to the necessity to model thin insulation between the parts of the core.

Here, a formulation based on the magnetic vector potential $\boldsymbol{A}$ and the current vector potential $\boldsymbol{T}$ is used, where $\boldsymbol{B} = \nabla \times \boldsymbol{A}$ and $\boldsymbol{J}_{\alpha\beta} = \nabla \times \boldsymbol{T}$ due to equations (3) and (4). Regarding the $\boldsymbol{J}_{\alpha\beta\gamma}$ component, it will not be directly modeled using potentials. However, as previously described, the weak formulation term related to $\boldsymbol{J}_{\alpha\beta\gamma}$ is approximately proportional to the weak formulation term associated with the magnetic induction $\boldsymbol{B}_{\alpha\beta}$. To achieve a symmetric system of equations, a time-primitive vector potential $\boldsymbol{\tau}$ is used instead of $\boldsymbol{T}$, where $\boldsymbol{T} = -\partial_t \boldsymbol{\tau} = -j\omega\boldsymbol{\tau}$. Potential $\boldsymbol{\tau}$ is interpolated by edge elements $\boldsymbol{N}_k$ (Bíró, 1999). Therefore, a thin layer of insulation between the parts of the multipart core is simply modeled by setting the interface condition $\nabla \times \boldsymbol{\tau} = 0$. Potential $\boldsymbol{A}$, interpolated by edge elements $\boldsymbol{N}_l$ is used to strongly ensure the continuity of the normal component of magnetic induction at the core/air interface.

Therefore, equations (21) and (22) turn into:

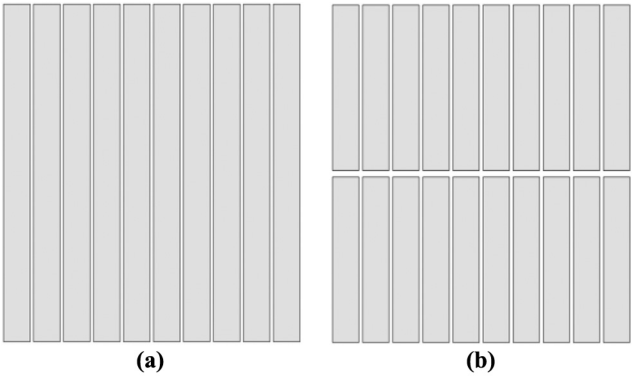

Figure 5.
Cross section comparison of two different open-type laminated cores

Notes: (a) A one-part core; (b) A two-part core
Source: Authors' own work

$$-j\omega\nabla \times \boldsymbol{\rho}\nabla \times \boldsymbol{\tau} + j\omega\nabla \times \boldsymbol{A} = 0 \tag{23}$$

$$\nabla \times \nu\nabla \times \boldsymbol{A} + j\omega\nabla \times \boldsymbol{\tau} = \boldsymbol{J}_{\alpha\beta\gamma} \tag{24}$$

In the region $\Omega_n = \Omega_0 \cup \Omega_s$ instead of equation (5) it follows:

$$\nabla \times \nu_0\nabla \times \boldsymbol{A} = \nabla \times \boldsymbol{T_s}, \tag{25}$$

where $\boldsymbol{J_s} = \nabla \times \boldsymbol{T_s}$ is due to equation (7).

Finally, using interpolation functions (edge elements) as weighting functions in equations (23)–(25), denoted by $\boldsymbol{N_m}$ and $\boldsymbol{N_n}$, the weak $\boldsymbol{A}\boldsymbol{\tau}\boldsymbol{A}$-formulation follows:

$$\begin{aligned}&\int_{\Omega_n} \nu_0\nabla \times \boldsymbol{A}\cdot\nabla \times \boldsymbol{N_m}d\Omega + \int_{\Omega_c} \boldsymbol{\nu}\nabla \times \boldsymbol{A}\cdot\nabla \times \boldsymbol{N_m}d\Omega + \\ &\int_{\Omega_c} \nabla \times j\omega\boldsymbol{\tau}\cdot\boldsymbol{N_m}d\Omega = \int_{\Omega} \boldsymbol{T}_0\cdot\nabla \times \boldsymbol{N_m}d\Omega\end{aligned} \tag{26}$$

$$\int_{\Omega_c} j\omega\boldsymbol{A}\cdot\nabla \times \boldsymbol{N_n}dV - \int_{\Omega_c} \boldsymbol{\rho}\nabla \times j\omega\boldsymbol{\tau}\cdot\nabla \times \boldsymbol{N_n}dV = 0, \tag{27}$$

where the index m represents the m-th degree of freedom for the $\boldsymbol{A}$ potential and the index n represents the n-th degree of freedom for the $\boldsymbol{\tau}$ potential (Frljic *et al.*, 2021).

6.1 Elimination of redundant degrees of freedom

As stated earlier, only the current density $\boldsymbol{J_{\alpha\beta}}$ is modeled directly, i.e. it holds that $\boldsymbol{J_{\alpha\beta}} = -j\omega\nabla \times \boldsymbol{\tau}$. Therefore, it is sufficient that $\boldsymbol{\tau} = \tau_\alpha\boldsymbol{a_\alpha} + \tau_\beta\boldsymbol{a_\beta} + \tau_\gamma\boldsymbol{a_\gamma}$ has only a γ-component (normal component), i.e. $\boldsymbol{\tau} = \tau_\gamma\boldsymbol{a_\gamma}$ and $\tau_{\alpha\beta} = \tau_\alpha\boldsymbol{a_\alpha} + \tau_\beta\boldsymbol{a_\beta} = 0$, where $\boldsymbol{a_\alpha}$, $\boldsymbol{a_\beta}$ and $\boldsymbol{a_\gamma}$ are unit vectors in α, β and γ directions according to the coordinate system in Figure 3. Also, the direction of the vector $\boldsymbol{a_\gamma}$ is represented with a red arrow in

Figure 6. Thus, the tangential component $\boldsymbol{\tau}_{\alpha\beta}$ is redundant and it is therefore desirable to eliminate it from the simulation.

If a structural mesh is created inside the core such that each edge of each finite element is either parallel to or perpendicular to $\boldsymbol{a}_\gamma$, it is possible to identify the tangential and normal components of the vector $\boldsymbol{\tau}$ with the edge degrees of freedom $\boldsymbol{\tau}_{\boldsymbol{k}}$, where $\boldsymbol{\tau} = \sum \tau_k \boldsymbol{N}_{\boldsymbol{k}}$. In that case, the product $\boldsymbol{N}_{\boldsymbol{k}} \cdot \boldsymbol{a}_\gamma$ is either 0 or $|\boldsymbol{N}_{\boldsymbol{k}}|$, for each edge of each finite element in Ω_c.

Therefore, using the rule:

$$\boldsymbol{N}_{\boldsymbol{k}} \cdot \boldsymbol{a}_\gamma = \begin{cases} 0, & \text{then } \tau_k = 0 \\ |\boldsymbol{N}_{\boldsymbol{k}}|, & \text{then } \tau_k = \tau_k \end{cases} \tag{28}$$

The redundant degrees of freedom from the matrix of coefficients in the preprocessing phase are eliminated. In Figure 6(a), the appropriate finite element and anisotropy vector $\boldsymbol{a}_\gamma$, represented by the red arrow, are presented. Using equation (28), the element shown in Figure 6(b) is obtained. By eliminating redundant degrees of freedom, the convergence speed of the simulation is significantly improved.

7. Verification

The simulation will be performed on an open-type four-part core model, with anisotropy directions equal to those shown in Figure 6(a). Each of the four parts of the core has dimensions 1 cm × 1 cm × 10 cm, that is, the core has overall dimensions 2 cm × 2 cm × 10 cm. Also, each part of the core has 27 laminations with a filling factor of $K_f = 0.94$. That means that the entire core consists of 108 laminations. The thickness of the laminations is $d = 0.35$ mm, the electrical resistivity is $\rho = 5 \cdot 10^{-7}$ Ωm and magnetic reluctivity is $\nu = 10^{-4}/\mu_0$. Field $\boldsymbol{T_s}$ is defined as the

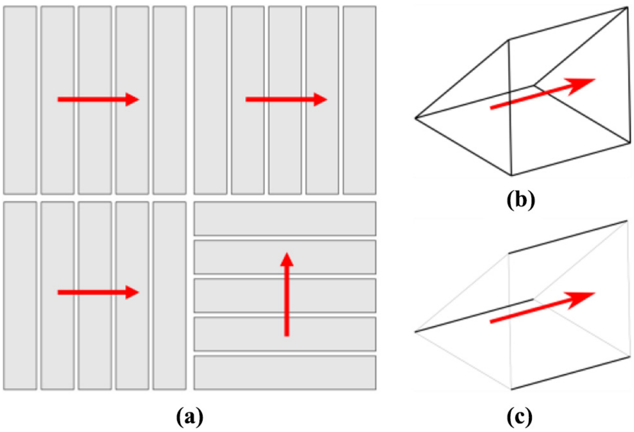

Notes: (a) Cross section of a laminated core. The red arrows represent the anisotropy vector for each of the four parts of the core; (b) A finite element with nine edges that are either parallel or perpendicular to the anisotropy vector (red arrow); (c) A finite element without edges to which redundant degrees of freedom are attached
Source: Authors' own work

Figure 6. Example of a multipart (four-part) open-type core

excitation. Field $\boldsymbol{T_s}$ corresponds to the density of the current $J_s = 2$ A/mm^2 flowing through the hollow cylinder (inner radius r = 2.5 cm, outer radius r = 4.5 cm and height h = 5 cm) positioned around the lower half of the core. The excitation frequency is $f = 50$ Hz.

7.1 2D simulation in the preprocessing phase

The simulation is performed over a cross section of a laminated core using a weak 2D $\boldsymbol{AT}$-formulation (Frljic and Trkulja, 2021). It is sufficient to carry out the simulation only over the part of the 2D domain that is covered by at least two finite elements of the 3D structural coarse mesh, provided that suitable boundary conditions are used, i.e. one element must contain edge effects and the other must be without edge effects. An example of simulation over a part of the 2D domain is shown in Figure 4(a), where the simulation surface covers four finite elements of the coarse mesh.

After the simulation was performed, two different values for the parameter κ were obtained using equation (20).

For elements that belong to the narrow edge of the laminations, it is valid that $\kappa = 5.69$, due to the appearance of edge effects. For the remaining elements, the value of this parameter is $\kappa = 6.39$, as shown in Figure 7.

The density of the 3D structural coarse mesh is 100 FEs per cross section of one part of the core, as seen in Figure 7(b), and in total 40,000 hexahedral FEs in the core and approximately 170,000 FEs in the rest of the domain. The density of the mesh in the 2D simulation is about 800 triangular FEs per surface of one finite element of the coarse mesh.

7.2 3D simulation results

A comparison of three different types of 3D FEM simulations for the calculation of eddy current losses over a given four-part open-type core model was made. The first type of simulation is the $\boldsymbol{AVA}$-type which uses the standard weak $\boldsymbol{AVA}$-formulation. The second type of simulation is $\boldsymbol{A\tau A}$*-type, which is based on the weak $\boldsymbol{A\tau A}$-formulation [equations (26) and (27)]. The third type of simulation is the $\boldsymbol{A\tau A}$-type which also uses the $\boldsymbol{A\tau A}$-formulation

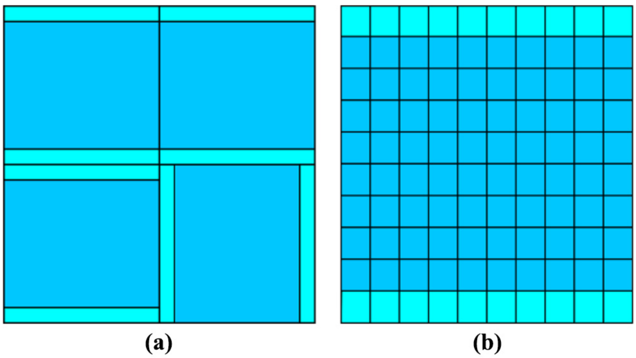

Notes: (a) Cross-sectional distribution in the entire four-part core. A lighter color corresponds to the value $\kappa = 5.69$ and a darker color corresponds to the value $\kappa = 6.39$; (b) projection of a 3D coarse mesh within one part of a multipart core
Source: Authors' own work

Figure 7.
Discrete distribution of parameter κ values

[equations (26) and (27)] but with the elimination of redundant degrees of freedom of the current vector potential $\boldsymbol{\tau}$. For the sake of comparability of the results, all three simulations were performed on the same mesh. The hardware used was an i3-3120M (2.5 GHz) CPU and 12 GB of RAM. Table 1 shows a comparison of three types of simulation. The amount of total losses P is equal in all three cases. $\boldsymbol{A\tau A^*}$-type and $\boldsymbol{A\tau A}$-type show an identical value of losses $P_{\alpha\beta\gamma}$ and $P_{\alpha\beta}$ which means that the elimination of redundant degrees of freedom does not affect the simulation result. The deviation between $\boldsymbol{AVA}$-type and $\boldsymbol{A\tau A}$-type is larger for $P_{\alpha\beta}$ losses and

Table 1. Comparison of three types of simulation for the calculation of eddy current losses in a four-part open-type laminated core

Type	P, mW	$P_{\alpha\beta\gamma}$, mW	$P_{\alpha\beta}$, mW	Time, s
AVA	168	110	58	2,840
$A\tau A^*$	165	108	57	8,220
$A\tau A$	165	108	57	2,250

Source: Authors' own work

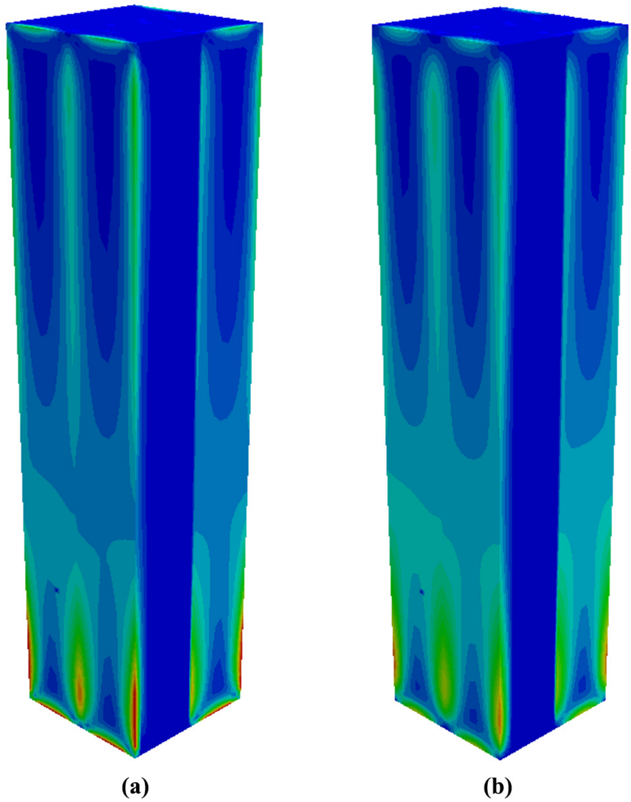

Notes: (a) AVA-type simulation results; (b) $A\tau A$-type simulation results
Source: Authors' own work

Figure 8. Distribution of total core losses

smaller for $P_{\alpha\beta\gamma}$ losses, which is expected because both formulations are based on the magnetic vector potential $\boldsymbol{A}$. We can see that the duration of the simulation is slightly better for $\boldsymbol{A\tau A}$-type than for $\boldsymbol{AVA}$-type and significantly better than for the $\boldsymbol{A\tau A}$*-type owing to the elimination of redundant degrees of freedom.

The distribution of total losses P obtained using $\boldsymbol{A\tau A}$-type and $\boldsymbol{AVA}$-type simulations are depicted in Figure 8.

8. Conclusion

Calculation of eddy current losses requires taking into account differences between the open-type core and the conventional core. As shown in Figure 8, using a multipart core reduces the size of the eddy current loops created by magnetic flux directed perpendicular to the surface of the lamination sheet. This lowers core losses.

The particularity of the geometry of the open-type core favors the use of a weak $\boldsymbol{A\tau A}$-formulation. Presented approach, with the elimination of redundant DOFs significantly improves the convergence speed. Numerical homogenization offers a simple way of taking into account edge effects for eddy currents induced by the magnetic flux tangential to the lamination surfaces. Comparison of the results shows good agreement with other possible approaches. Proposed method, which yields accurate results, can easily be implemented and used for optimization when designing open-type cores.

References

Bíró, O. (1999), "Edge element formulations of eddy current problems", *Computer Methods in Applied Mechanics and Engineering*, Vol. 169 Nos 3/4, pp. 391-405, doi: 10.1016/S0045-7825(98)00165-0.

Bíró, O., Preis, K. and Ticar, I. (2005), "A FEM method for eddy current analysis in laminated media", *COMPEL - The International Journal for Computation and Mathematics in Electrical and Electronic Engineering*, Vol. 24 No. 1, pp. 241-248, doi: 10.1108/03321640510571264.

De Gersem, H., Vanaverbeke, S. and Samaey, G. (2012), "Three-dimensional-two-dimensional coupled model for eddy currents in laminated iron cores", *IEEE Transactions on Magnetics*, Vol. 48 No. 2, pp. 815-818, doi: 10.1109/TMAG.2011.2172924.

Dular, P., Gyselinck, J., Geuzaine, C., Sadowski, N. and Bastos, J.P.A. (2003), "A 3-D magnetic vector potential formulation taking eddy currents in lamination stacks into account", *IEEE Transactions on Magnetics*, Vol. 39 No. 3, pp. 1424-1427, doi: 10.1109/TMAG.2003.810386.

Frljic, S. and Trkulja, B. (2021), "Two-step method for the calculation of eddy current losses in an open-core transformer", *IEEE Transactions on Magnetics*, Vol. 57 No. 3, pp. 1-8, doi: 10.1109/TMAG.2020.3044876.

Frljic, S., Trkulja, B. and Žiger, I. (2021), "Calculation of the eddy current losses in a laminated open-type transformer core based on the $A\rightarrow$, $T\rightarrow - A\rightarrow$ formulation", *Applied Sciences*, Vol. 11 No. 23, p. 11543, doi: 10.3390/APP112311543.

Gyselinck, J., Vandevelde, L., Melkebeek, J., Dular, P., Henrotte, F. and Legros, W. (1999), "Calculation of eddy currents and associated losses in electrical steel laminations", *IEEE Transactions on Magnetics*, Vol. 35 No. 3, pp. 1191-1194, doi: 10.1109/20.767162.

Hanser, V., Schobinger, M. and Hollaus, K. (2022), "Efficient computation of eddy current losses in laminated cores with air gaps by the multiscale FEM", *2022 23rd Int. Conf. Comput. Electromagn. Fields, COMPUMAG 2022*, doi: 10.1109/COMPUMAG55718.2022.9827497.

Henrotte, F., Steentjes, S., Hameyer, K. and Geuzaine, C. (2015), "Pragmatic two-step homogenisation technique for ferromagnetic laminated cores", *IET Science, Measurement and Technology*, Vol. 9 No. 2, pp. 152-159, doi: 10.1049/iet-smt.2014.0201.

Hollaus, K. and Schöberl, J. (2015), "Multi-scale FEM and magnetic vector potential A for 3D eddy currents in laminated media", *COMPEL - The International Journal for Computation and Mathematics in Electrical and Electronic Engineering*, Vol. 34 No. 5, pp. 1598-1608, doi: 10.1108/COMPEL-02-2015-0090.

Hollaus, K. and Schoberl, J. (2018), "Some 2-D multiscale finite-element formulations for the eddy current problem in iron laminates", *IEEE Transactions on Magnetics*, Vol. 54 No. 4, pp. 1-16, doi: 10.1109/TMAG.2017.2777395.

Kaimori, H., Kameari, A. and Fujiwara, K. (2007), "FEM computation of magnetic field and iron loss in laminated iron core using homogenization method", *IEEE Transactions on Magnetics*, Vol. 43 No. 4, pp. 1405-1408, doi: 10.1109/TMAG.2007.892429.

Lapthorn, A. and Keenan, K. (2015), "A radially laminated core for partial core transformers".

Liew, M.C. and Bodger, P.S. (2001), "Partial-core transformer design using reverse modelling techniques", *IEE Proceedings – Electric Power Applications*, Vol. 148 No. 6, pp. 513-520, doi: 10.1049/IP-EPA:20010587.

Niyonzima, I., Sabariego, R.V., Dular, P., Henrotte, F. and Geuzaine, C. (2013), "Computational homogenization for laminated ferromagnetic cores in magnetodynamics", *IEEE Transactions on Magnetics*, Vol. 49 No. 5, pp. 2049-2052, doi: 10.1109/TMAG.2012.2237546.

Ziger, I., Bojanic, B. and Krajtner, D. (2014), "Open-core power voltage transformer: concept, properties, application", *IEEE Int. Energy Conf.*, May 2014, pp. 246-253, doi: 10.1109/ENERGYCON.2014.6850436.

Ziger, I., Trkulja, B. and Stih, Z. (2018), "Determination of core losses in open-core power voltage transformers", *IEEE Access*, Vol. 6, pp. 29426-29435, doi: 10.1109/ACCESS.2018.2838446.

Corresponding author
Stjepan Frljić can be contacted at: stjepan.frljic@fer.hr